

# Tunnelling Effects on the 1,3- and 1,5-Sigmatropic Hydrogen Shifts in the Ground State of Photo-Fries Rearranged Intermediates of Phenyl Acetate Studied by Laser Flash Photolysis

Tadashi Arai, Seiji Tobita, and Haruo Shizuka\*

Contribution from the Department of Chemistry, Gunma University, Kiryu, Gunma 376, Japan

Received November 14, 1994<sup>®</sup>

**Abstract:** The rate constants for the 1,3- and 1,5-sigmatropic hydrogen shifts in the ground state of the photo-Fries rearranged intermediates of phenyl acetate produced by laser flash photolysis at 266 nm were directly measured in several solvents. The rate constant for the intramolecular 1,3-hydrogen shift ( $3.6 \text{ s}^{-1}$ ) is greater than that for the 1,5-hydrogen shift ( $6.5 \times 10^{-2} \text{ s}^{-1}$ ) in the ground state in methylcyclohexane (MCH) at 293 K, contrary to the expectation by the Woodward–Hoffmann rule, showing that the heteroatom of the corresponding carbonyl oxygen plays an important role for the intramolecular hydrogen shifts. On the basis of the experimental results of temperature and isotope effects, it is shown that the intramolecular 1,3-hydrogen (or deuterium) shift in MCH proceeds via tunnelling processes at two vibrational energy levels:  $E = 0$  ( $\nu = \nu_0$ ) and  $E = E_\nu$  ( $= 3.9 \text{ kcal mol}^{-1}$  for the hydrogen shift or  $4.4 \text{ kcal mol}^{-1}$  for the deuterium shift) ( $\nu = \nu_1$ ) under the experimental condition. The temperature and isotope effects on the 1,3-shifts can be elucidated by the calculated rates according to the tunnel effect theory proposed by Formosinho. The enhancement of the rates for the 1,3- and 1,5-sigmatropic shifts in polar solvents, especially in alcohols, is caused intermolecularly by a basic catalysis of the solvents. It is shown that the 1,3- or 1,5-sigmatropic hydrogen shift proceeds via the intramolecular process at a low concentration of phenyl acetate ( $\sim 2 \times 10^{-3} \text{ M}$ ) in nonpolar MCH.

## Introduction

Sigmatropic hydrogen shift is one of the most important and elementary processes in both chemistry and biochemistry. The intramolecular hydrogen shift is of particular interest in connection with the Woodward–Hoffmann rule.<sup>1,2</sup> Until recently, a number of theoretical<sup>3–7</sup> and experimental<sup>8–14</sup> studies on the intramolecular hydrogen shifts both in the ground and excited states have been reported.

The photo-Fries rearrangements are typical reactions which involve 1,3- and 1,5-sigmatropic hydrogen shifts in the electronically ground state. Since the original work by Anderson

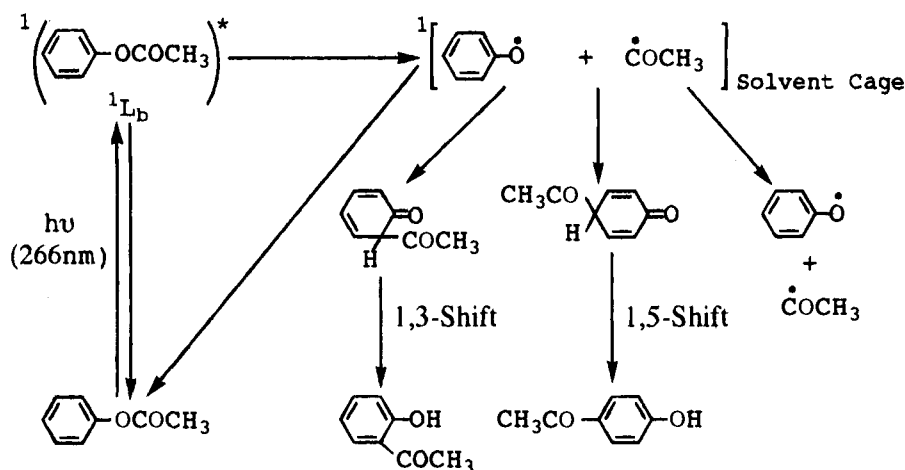
and Reese,<sup>15</sup> a number of studies on the photo-Fries rearrangements have been reported.<sup>16–31</sup> It has been shown that (1) the  $\beta$ -bond fission of phenyl acetate (PAH) (or acetanilide) takes place from the excited singlet state  $^1(\pi, \pi^*)$   $^1L_b$ ,<sup>18,22</sup> (2) The resultant radical pairs in a solvent cage rapidly recombine to give the starting molecules, ortho and para-rearranged products.<sup>20,22</sup> (3) The radicals escape in part ( $\sim 10\%$ ) from the solvent cage (Scheme 1).<sup>20,22</sup> (4) The reaction quantum yields of PAH in cyclohexane at 254 nm at 293 K are known to be 0.16 (*o*-hydroxyacetophenone), 0.15 (*p*-hydroxyacetophenone), and 0.06 (phenol).<sup>22</sup>

The mechanism in Scheme 1 has been confirmed by CIDNP experiments,<sup>26,27</sup> conventional flash photolysis in the condensed

- <sup>®</sup> Abstract published in *Advance ACS Abstracts*, April 1, 1995.
- (1) Woodward, R. B.; Hoffmann, R. *J. Am. Chem. Soc.* **1965**, *87*, 2511.
  - (2) Fleming, I. *Frontier Orbitals and Organic Chemical Reactions*; Wiley: New York, 1976.
  - (3) Evansack, J. D.; Houk, K. N. *J. Phys. Chem.* **1990**, *94*, 5518.
  - (4) Dorigo, A. E.; McCarrick, M. A.; Loncharich, R. J.; Houk, K. N. *J. Am. Chem. Soc.* **1990**, *112*, 7508.
  - (5) Bernardi, F.; Olivucci, M.; Robb, M. A.; Tonachini, G. *J. Am. Chem. Soc.* **1992**, *114*, 5805.
  - (6) Sobolewski, A. L. *Chem. Phys. Lett.* **1993**, *211*, 293.
  - (7) Tapia, O.; Andrés, J.; Safont, V. S. *J. Phys. Chem.* **1994**, *98*, 4821.
  - (8) Duhaime, R. M.; Weedon, A. C. *Can. J. Chem.* **1987**, *65*, 1867.
  - (9) Grellmann, K. H.; Weller, H.; Tauer, E. *Chem. Phys. Lett.* **1983**, *95*, 195.
  - (10) Al-Soufi, W.; Grellmann, K. H.; Nickel, B. *J. Phys. Chem.* **1991**, *95*, 10503.
  - (11) Al-Soufi, W.; Eychmüller A.; Grellmann, K. H. *J. Phys. Chem.* **1991**, *95*, 2022.
  - (12) Reid, P. J.; Wickham, S. D.; Mathies, R. A. *J. Phys. Chem.* **1992**, *96*, 5720.
  - (13) Liu, M. T. H.; Bonneau, R. *J. Am. Chem. Soc.* **1992**, *114*, 3604; Liu, M. T. H. *Acc. Chem. Res.* **1994**, *27*, 287.
  - (14) Sekiguchi, T.; Yamaji, M.; Tatemitsu, H.; Sakata, Y.; Shizuka, H. *J. Phys. Chem.* **1993**, *97*, 7003.

- (15) Anderson, J. C.; Reese, C. B. *Proc. Chem. Soc.* **1960**, 217; *J. Chem. Soc.* **1963**, 1781.
- (16) Kobsa, H. *J. Org. Chem.* **1962**, *27*, 2293.
- (17) Elad, D.; Rao, D. V.; Stenberg, V. I. *J. Org. Chem.* **1965**, *30*, 3252.
- (18) Shizuka, H.; Tanaka, I. *Bull. Chem. Soc. Jpn.* **1968**, *41*, 2343.
- (19) Shizuka, H. *Bull. Chem. Soc. Jpn.* **1969**, *42*, 52.
- (20) Shizuka, H. *Bull. Chem. Soc. Jpn.* **1969**, *42*, 57.
- (21) Shizuka, H.; Tanaka, I. *Bull. Chem. Soc. Jpn.* **1969**, *42*, 909.
- (22) Shizuka, H.; Morita, T.; Mori, Y.; Matsui, K. *Bull. Chem. Soc. Jpn.* **1969**, *42*, 1831.
- (23) Shizuka, H.; Kanai, T.; Morita, T.; Ohto, Y.; Tanaka, I. *Tetrahedron* **1971**, *27*, 4021.
- (24) Bellus, D. *Advances in Photochemistry*; John Wiley & Sons: New York, 1971; Vol. 8, p 109.
- (25) Meyer, J. W.; Hammond, G. S. *J. Am. Chem. Soc.* **1970**, *92*, 2187; **1972**, *94*, 2219.
- (26) Adam, W. *Chem. Commun.* **1974**, 289.
- (27) Adam, W.; de Sanabia, J. A.; Fischer, H. *J. Org. Chem.* **1973**, *38*, 2571.
- (28) Kalmus, C. E.; Hercules, D. M. *Tetrahedron Lett.* **1972**, 1575; *J. Am. Chem. Soc.* **1974**, *96*, 449.
- (29) Humphrey, J. S., Jr.; Roller, R. S. *Mol. Photochem.* **1971**, *3*, 35.
- (30) Beck, S. M.; Brus, L. E. *J. Am. Chem. Soc.* **1982**, *104*, 1805.
- (31) Ghibaldi, E.; Colussi, A. *Chem. Phys. Lett.* **1983**, *94*, 121.

## Scheme 1



phase,<sup>28,29</sup> gas phase photolysis<sup>21,25</sup> and the detection of transient intermediates by spontaneous Raman spectroscopy.<sup>30</sup> Furthermore, a disproportionation reaction between acetyl and phenoxy radicals in a solvent cage to form phenol and ketene was suggested by Ghibaudi and Colussi.<sup>31</sup>

In a preliminary paper,<sup>32</sup> we have reported direct measurements of 1,3- and 1,5-sigmatropic hydrogen shifts in the electronic ground state of photo-Fries rearranged intermediates of PAH by means of laser flash photolysis. The rate of 1,3-hydrogen shift in MCH is faster than that of 1,5-hydrogen shift on the contrary to the expectation by the Woodward–Hoffmann rule.

In the present paper, the isotope and temperature effects on the 1,3- and 1,5-sigmatropic shifts of the photo-Fries rearranged intermediates were examined by means of laser flash photolysis, and the theoretical consideration was made according to the tunnel effect theory proposed by Formosinho,<sup>33–38</sup> in order to clarify the reaction mechanism.

## Experimental Section

Phenyl acetate (PAH; Aldrich) was washed with aqueous 5% Na<sub>2</sub>CO<sub>3</sub> and then with saturated aqueous CaCl<sub>2</sub>, dried with CaSO<sub>4</sub>, and fractionally distilled under reduced pressure. Phenyl acetate-*d*<sub>5</sub> (PAD) was prepared by the reaction of phenol-*d*<sub>6</sub> (Aldrich) with anhydrous acetic acid and purified in a similar manner. Methylcyclohexane (MCH; Aldrich spectrophotometric grade) was dried with CaH<sub>2</sub> and purified by distillation. Acetonitrile (ACN; Wako spectroscopic) was dried with molecular sieves 4A and distilled from P<sub>2</sub>O<sub>5</sub>. Traces of P<sub>2</sub>O<sub>5</sub> were then removed by distillation from anhydrous K<sub>2</sub>CO<sub>3</sub>. Methanol (MeOH; Wako spectroscopic), ethanol (EtOH; Wako spectroscopic), 1-propanol (1-PrOH; Wako special grade) and isopropyl alcohol (*i*-PrOH; Wako spectroscopic) were distilled from CaH<sub>2</sub>. Diethyl ether (DEE; Wako spectroscopic) was shaken with ferrous sulfate and concentrated H<sub>2</sub>SO<sub>4</sub>, then washed with water, dried with CaCl<sub>2</sub>, and distilled. Tetrahydrofuran (THF; Wako spectroscopic) was purified by distillation from LiAlH<sub>4</sub>.

A nanosecond Nd<sup>3+</sup>:YAG laser at 266 nm (JK-LASERS HY 500, pulse width 8 ns, 20 mJ pulse<sup>-1</sup> cm<sup>-2</sup>) was used for excitation. The monitoring system consisted of a 150W xenon lamp. The transient signals were recorded on a digitizing oscilloscope (Tektronix, TDS-540) and transferred to a personal computer (NEC, PC-9821Ap). The fluctuation in the intensity of the xenon lamp during time trace

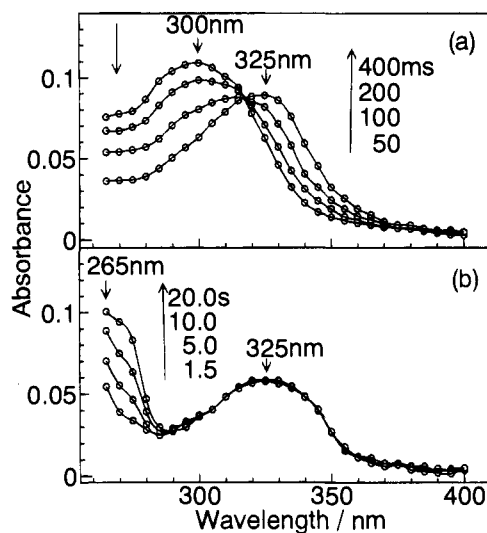


**Figure 1.** Time-resolved transient absorption spectra obtained by 266 nm laser flash photolysis of PAH ( $\sim 5 \times 10^{-3}$  M) in MCH at 293 K: (a) delay time, 50–400 ms and (b) delay time, 1.5–20 s.

measurements was recorded simultaneously on another channel of the oscilloscope, and the base correction was made. Details for the laser photolysis system were reported elsewhere.<sup>39</sup>

Fresh samples were used for the laser photolysis to avoid the accumulation of photochemical products. The kinetic measurements were carried out by using a 10 mm quartz cell. For measurements of the 1,5-hydrogen and 1,3-deuterium shifts in MCH, a 1 mm quartz cell was used to prevent the effect of diffusion on the rise rate. It was confirmed that the effect of dissolved oxygen on the rates for the hydrogen and deuterium shifts was negligible. Therefore, all the experiments were carried out under aerated condition.

Molecular orbital calculations were performed by use of the PM3 method<sup>40</sup> on the "PASOCON MOPAC/386" which was based on the MOPAC (V5.0 QCPE No. 455) of TORAY SYSTEM CENTER.

## Results and Discussion

**Intramolecular Hydrogen Shifts of Photo-Fries Rearranged Intermediates.** Direct measurements of the rates for the 1,3- and 1,5-hydrogen shifts were carried out in methylcyclohexane, MCH at 293 K. Figure 1a shows the transient absorption spectra obtained by 266 nm laser flash photolysis of PAH ( $5.0 \times 10^{-3}$  M) in MCH. With a lapse in time an absorption peak at 325 nm appears with a decrease of the peak

(32) Arai, T.; Tobita, S.; Shizuka, H. *Chem. Phys. Lett.* **1994**, *223*, 521.

(33) Formosinho, S. J. *J. Chem. Soc., Faraday Trans. 2* **1976**, *72*, 1313.

(34) Formosinho, S. J.; Arnaut Luis, G. *Advances in Photochemistry*; John Wiley & Sons: New York, 1991; Vol. 16.

(35) Formosinho, S. J. *Mol. Photochem.* **1976**, *7*, 41.

(36) Formosinho, S. J. *J. Chem. Soc., Faraday II* **1974**, *70*, 605.

(37) Formosinho, S. J.; da Silva, J. D. *Mol. Photochem.* **1974**, *6*, 409.

(38) Formosinho, S. J. In *Excited States of Biological Molecules*; Birks, J. B., Ed.; Wiley, 1975; p 555.

(39) Yamaji, M.; Aihara, Y.; Itoh, T.; Tobita, S.; Shizuka, H. *J. Phys. Chem.* **1994**, *98*, 7014.

(40) Stewart, J. J. P. *J. Comput. Chem.* **1989**, *10*, 209, 221.

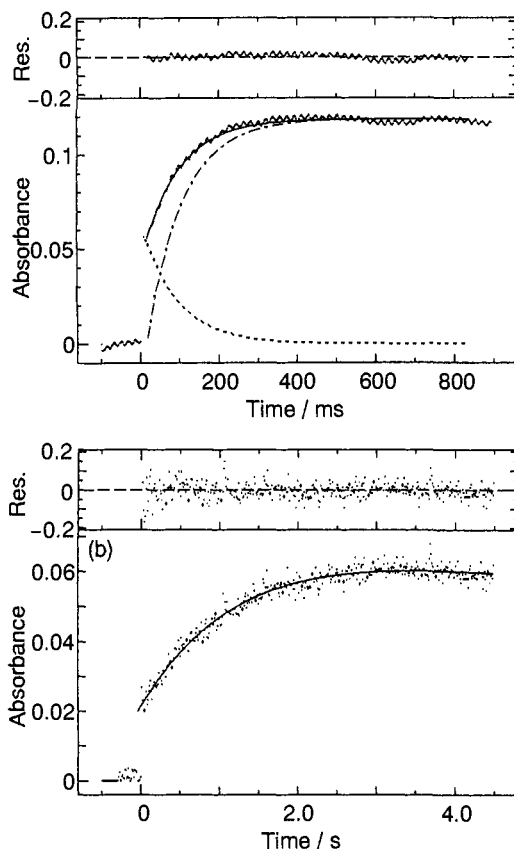


**Figure 2.** (a) The time trace of the transient absorption of PAH in MCH monitored at 325 nm. (b) The time trace of the transient absorption of PAH in MCH monitored at 265 nm. For details, see text.

around 300 nm. The transient absorption peak around 325 nm is ascribable to the absorption of ortho-final product, *o*-hydroxyacetophenone.<sup>22</sup> The existence of an isosbestic point at 318 nm demonstrates that the 300 nm band corresponds to the absorption band of the ortho-rearranged intermediate (Scheme 1). The shape and position of the transient spectra are in good agreement with those reported by Kalmus et al.<sup>28</sup> The formation rate of ortho-final product was determined by measuring the rise time at 325 nm. In other words, this corresponds to the rate of the 1,3-hydrogen shift. Figure 2a shows a typical time trace of the ortho-final product monitored at 325 nm in MCH at 293 K. Since the absorption at 325 nm is a superposition between those of ortho-rearranged intermediate and ortho product, the time trace can be analyzed by a composite function with rise and decay components. Therefore, the observed rate is represented by eq 1

$$A_{1,3}(t) = A \exp(-k_{1,3}t) + A'(1 - \exp(-k'_{1,3}t)) \quad (1)$$

where  $A_{1,3}(t)$  is the observed absorbance at 325 nm,  $A$  is the initial absorbance of the ortho-rearranged intermediate,  $A'$  is the final absorbance of ortho-final product, and  $k_{1,3}$  and  $k'_{1,3}$  are the decay and rise rate constants of ortho-rearranged intermediate and ortho-final product, respectively. By the least-square fitting of eq 1 to the rise curve in Figure 2a,  $k_{1,3}$  and  $k'_{1,3}$  were determined to be  $7.2(\pm 1.0)$  and  $7.1(\pm 1.0) \text{ s}^{-1}$  in MCH ([PAH] =  $5 \times 10^{-3} \text{ M}$ ) at 293 K, respectively, showing  $k_{1,3} \approx k'_{1,3}$ . In Figure 2a, the solid line displays the best fitted line calculated by eq 1, and the broken and dot broken lines are the best fitted lines calculated by the first and second terms in eq 1, respectively. To confirm that the observed rate constant of hydrogen atom transfer corresponds to that of intramolecular process, the effect of parent molecule concentration [PAH] on

the formation rate of the ortho product was examined. The rate of the 1,3-hydrogen shift depended on [PAH], suggesting that the intermolecular interaction of ortho intermediate with the starting material, PAH, participates the hydrogen atom transfer as shown in eq 2<sup>32</sup>

$$k_{1,3}^{\text{H}} = (k_{1,3}^{\text{H}})_0 + (k_{1,3}^{\text{H}})_{\text{se}}[\text{PAH}] \quad (2)$$

where  $(k_{1,3}^{\text{H}})_0$  and  $(k_{1,3}^{\text{H}})_{\text{se}}$  denote the intrinsic rate constant for the intramolecular 1,3-hydrogen shift and the self-enhanced 1,3-hydrogen shift by the starting molecule, PAH. The rate constants of  $(k_{1,3}^{\text{H}})_0$  and  $(k_{1,3}^{\text{H}})_{\text{se}}$  of the intramolecular 1,3-hydrogen shift in MCH at 293 K were determined to be  $3.6(\pm 0.6) \text{ s}^{-1}$  and  $3.3 \times 10^2 \text{ M}^{-1} \text{ s}^{-1}$ , respectively. To clarify the concentration effect of the rearranged intermediate on the 1,3-hydrogen shift, the kinetic measurements were carried out under various laser intensities. However, the concentration effect of the ortho-rearranged intermediate on the rate could not be detected under the present experimental condition (up to  $40 \text{ mJ pulse}^{-1} \text{ cm}^{-2}$ ). The rate constant ( $3.6(\pm 0.6) \text{ s}^{-1}$ ) obtained for the 1,3-hydrogen shift was about three times greater than that ( $1.25 \text{ s}^{-1}$ ) reported by Kalmus et al.<sup>28</sup>

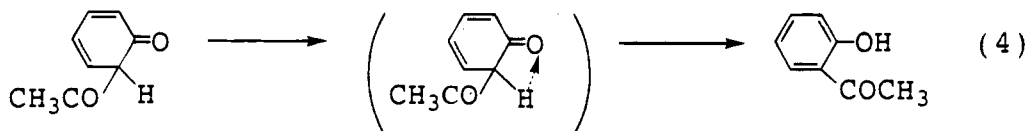
After the complete rise of the absorption peak around 325 nm, a new absorption band around 265 nm appears as shown in Figure 1b. The 265 nm band can be assigned to the absorption band of para-final product, *p*-hydroxyacetophenone.<sup>22</sup> The time trace monitored at 265 nm (in Figure 1b) in MCH at 293 K is shown in Figure 2b. The fast rise component is due to the absorption of *o*-hydroxyacetophenone. The rate constant ( $k_{1,5}^{\text{H}}$ ) of 1,5-hydrogen shift was determined by direct fitting of the rise curve monitored at 265 nm after the complete formation of ortho-rearranged product. There was a slight concentration effect of PAH on  $k_{1,5}$ .<sup>32</sup> The rate of  $k_{1,5}$  was given by

$$k_{1,5}^{\text{H}} = (k_{1,5}^{\text{H}})_0 + (k_{1,5}^{\text{H}})_{\text{se}}[\text{PAH}] \quad (3)$$

where  $(k_{1,5}^{\text{H}})_0$  and  $(k_{1,5}^{\text{H}})_{\text{se}}$  denote the intrinsic rate constant for the intramolecular 1,5-hydrogen shift and the self-enhanced 1,5-hydrogen shift by the starting material, PAH. The rate constants of 1,5-hydrogen shift ( $k_{1,5}^{\text{H}})_0$  and  $(k_{1,5}^{\text{H}})_{\text{se}}$  were determined to be  $6.5(\pm 0.6) \times 10^{-2} \text{ s}^{-1}$  and  $2.8 \text{ M}^{-1} \text{ s}^{-1}$ , respectively, by measuring the concentration dependence of  $k_{1,5}^{\text{H}}$ .

The Woodward–Hoffmann rule is usually applied to sigma-tropic shifts in pure  $\pi$ -electron systems of the carbon framework in which the orbital interactions play a dominant role.<sup>1,2</sup> In the present system, however, the ortho and para-intermediates have a heteroatom (carbonyl–oxygen atom) as the reactive position, so that the nonbonding electrons on the corresponding carbonyl–oxygen atom may play an important role for the hydrogen shifts. For example, the intramolecular 1,3-hydrogen shift in the ground state can be depicted by eq 4. It is important to note that the hydrogen atom involved in the hydrogen shifts does not separate from the ortho or para-rearranged intermediate considering that there is no oxygen effect on the rates.

The isotope effect on the hydrogen shifts was examined by use of phenyl acetate- $d_5$  (PAD). Figure 3 shows the transient absorption spectra obtained by 266 nm laser photolysis of PAD ( $5 \times 10^{-3} \text{ M}$ ) in MCH at 293 K. The peaks of the transient spectra are similar to those of PAH. With a decrease in the peak around 300 nm an absorption peak at 325 nm appears with a lapse in time. The bands around 300 and 325 nm are those of ortho-rearranged intermediate- $d_5$  and final product- $d_5$ , respectively. The rate ( $k_{1,3}^{\text{D}}$ ) of the 1,3-deuterium shift can be also given by



$$k_{1,3}^D = (k_{1,3}^D)_0 + (k_{1,3}^D)_{se}[PAD] \quad (5)$$

where  $(k_{1,3}^D)_0$  and  $(k_{1,3}^D)_{se}$  denote the intrinsic rate constant for intramolecular 1,3-deuterium shift and the self-enhanced rate constant for the 1,3-deuterium shift by the starting material, PAD, respectively. The values of  $(k_{1,3}^D)_0$  and  $(k_{1,3}^D)_{se}$  were obtained to be  $9.5(\pm 0.6) \times 10^{-1} \text{ s}^{-1}$  and  $8.6(\pm 1.0) \times 10 \text{ M}^{-1} \text{ s}^{-1}$ , respectively. The rate of the 1,5-deuterium shift was too slow to determine the intramolecular rate constant  $(k_{1,5}^D)_0$  by laser photolysis, since the small value of  $(k_{1,5}^D)_0$  was completely masked with that of  $(k_{1,5}^D)_{se}[PAD]$  even at a low concentration of PAD ( $2 \times 10^{-3} \text{ M}$ ). The kinetic isotope effect of  $(k_{1,3}^H)_0 / (k_{1,3}^D)_0$  was obtained as 3.8 at 293 K. The intrinsic rate constants  $(k_{1,3}^H)_0$ ,  $(k_{1,5}^H)_0$ , and  $(k_{1,3}^D)_0$  in nonpolar MCH are listed in Table 1.

**Solvent Effects on the 1,3- and 1,5-Sigmatropic Hydrogen and Deuterium Shifts.** The solvent effects on the sigmatropic shifts were examined in various solvents. Figure 4 shows the transient absorption spectra obtained by 266 nm laser flash photolysis of PAH in a polar solvent of ACN at 293 K. As shown in the case of MCH, the absorption band at around 300 nm decays with the appearance of a 325 nm band due to the formation of the ortho-rearranged product along with the isosbestic point at 315 nm. In contrast to the transient spectra in MCH, the formation of the ortho and para-rearranged products in ACN is completed within almost the same time range. The absorption peak at 270 nm is due to para-final product, *p*-hydroxyacetophenone.<sup>22</sup> The rate constants of the 1,3- and 1,5-hydrogen shifts were determined by measurements of the rise rates at 325 and 270 nm. The  $k_{obs}$  value in ACN also showed a slight concentration dependence, and the rate constants of the 1,3- and 1,5-hydrogen shifts ( $(k_{1,3}^H)_0$  and  $(k_{1,5}^H)_0$ ) in ACN were determined to be  $5.0(\pm 1.0) \times 10$  and  $1.2(\pm 0.4) \times 10^2 \text{ s}^{-1}$ , respectively, from the plots similar to those in MCH. The rates for the 1,3- and 1,5-hydrogen shifts become considerably fast in polar ACN in comparison with those in nonpolar MCH. The  $k_{se}$  values for 1,3- and 1,5-hydrogen shifts in ACN were  $5.3 \times 10^3$  and  $1.1 \times 10^4 \text{ M}^{-1} \text{ s}^{-1}$ , respectively. Both the values of  $(k_{1,5}^H)_0$  and  $(k_{1,5}^H)_{se}$  for the 1,5-hydrogen shift in ACN were about two times greater than those of  $(k_{1,3}^H)_0$  and  $(k_{1,3}^H)_{se}$  for the 1,3-hydrogen shift. The enhancement of the value of  $k_{1,3}^H$  or  $k_{1,5}^H$  may be due to an intermolecular interaction between the corresponding intermediate and polar ACN molecule(s).

The rate constants of hydrogen and deuterium shifts in diethyl ether (DEE) or tetrahydrofuran (THF) were measured by 266

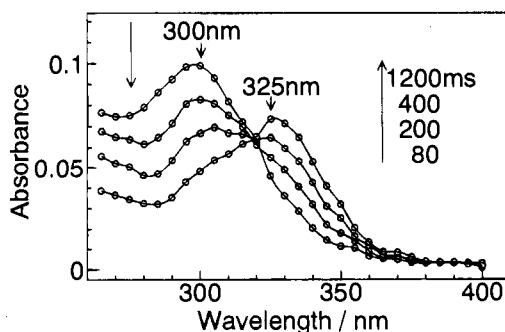


**Figure 3.** Time-resolved transient absorption spectra obtained by 266 nm laser flash photolysis of PAD ( $\sim 5 \times 10^{-3} \text{ M}$ ) in MCH at 293 K; delay time, 80–1200 ms.

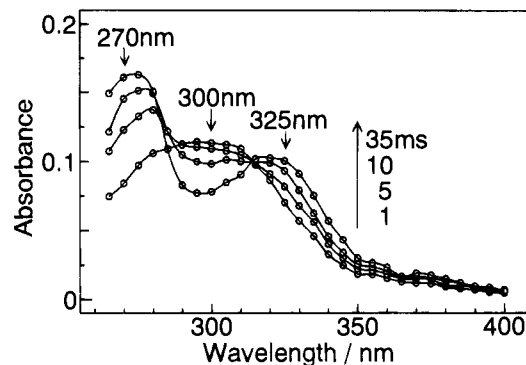


**Figure 4.** Time-resolved transient absorption spectra obtained by 266 nm laser flash photolysis of PAH ( $\sim 5 \times 10^{-3} \text{ M}$ ) in ACN at 293 K; delay time, 1–35 ms.

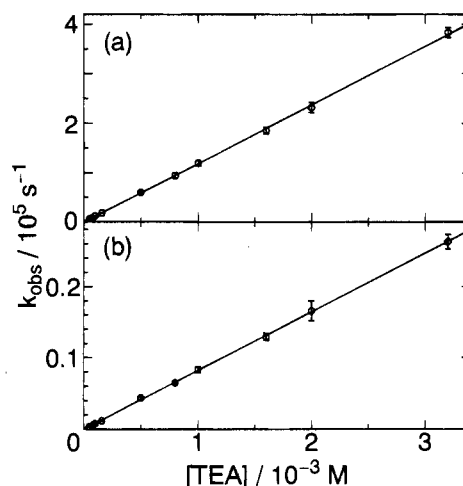


**Figure 5.** The plots of the observed formation rates of (a) ortho- and (b) para-rearranged products from PAH in MCH as a function of [TEA].

nm laser flash photolysis of PAH or PAD at a relatively low concentration ( $\sim 2 \times 10^{-3} \text{ M}$ ), in order to avoid the self-enhanced hydrogen shifts. The results are also listed in Table 1. The rate constant of 1,3-hydrogen shift is greater than that of 1,5-hydrogen shift in DEE or THF.

In alcohols such as methanol (MeOH), ethanol (EtOH), 1-propanol (1-PrOH), and isopropyl alcohol (*i*-PrOH), the rates for both 1,3- and 1,5-sigmatropic shifts become drastically fast ( $\sim 10^5 \text{ s}^{-1}$ ). It was confirmed that there was no self-enhancement effect on the hydrogen shifts in alcohols. This may be due to the fact that the interaction between the rearranged intermediates and alcohol molecules is significantly effective for the hydrogen atom transfer in comparison with that between the intermediates and the starting material. To reveal the solvent effect of alcohols on the hydrogen shifts, we examined the effect of triethylamine (TEA) on the hydrogen shifts in nonpolar MCH ( $[PAH] = 2 \times 10^{-3} \text{ M}$ ) at 293 K. The observed rates for 1,3 and 1,5-hydrogen shifts are shown in Figure 5 (parts a and b, respectively).

The rates for both 1,3- and 1,5-hydrogen shifts increase linearly with increasing [TEA] as follows:

$$k_{1,3}^{obs} = (k_{1,3}^H)_0 + (k_{1,3}^H)_e[TEA] \quad (6)$$

$$k_{1,5}^{\text{obs}} = (k_{1,5}^{\text{H}})_0 + (k_{1,5}^{\text{H}})_e[\text{TEA}] \quad (7)$$

where  $(k_{1,3}^{\text{H}})_0$  and  $(k_{1,5}^{\text{H}})_0$  are the rate constants for 1,3- and 1,5-hydrogen shifts in MCH (see Table 1). The rate constants,  $(k_{1,3}^{\text{H}})_e$  and  $(k_{1,5}^{\text{H}})_e$ , for the TEA enhancements of 1,3- and 1,5-hydrogen shifts for PAH were determined as  $1.2 \times 10^8$  and  $8.2 \times 10^6 \text{ M}^{-1} \text{ s}^{-1}$ , respectively. Similar experiments were carried out by use of PAD ( $2 \times 10^{-3} \text{ M}$ ) in MCH in the presence of TEA, and the values of the rate constants for  $(k_{1,3}^{\text{D}})_e$  and  $(k_{1,5}^{\text{D}})_e$ , enhanced by TEA were obtained to be  $2.9 \times 10^7$  and  $1.3 \times 10^6 \text{ M}^{-1} \text{ s}^{-1}$ , respectively.

On the other hand, we measured the rates of the 1,3- and 1,5-hydrogen shifts in trifluoroethanol (TFE) as a typical acidic solvent. The rate constants of the 1,3- and 1,5-hydrogen shifts at  $[\text{PAH}] = 2 \times 10^{-3} \text{ M}$  in TFE were obtained to be  $3.0(\pm 1.2) \times 10$  and  $8.2(\pm 1.1) \times 10 \text{ s}^{-1}$ , respectively. The rate constants of 1,3- and 1,5-sigmatropic hydrogen shifts in TFE were very small compared to those in usual alcohols as can be seen in Table 1. It can be said that usual alcohols act as a basic catalysis but not as an acidic catalysis. The basic catalysis of the amines can be accounted for by eqs 8a and b where (a) and (b) correspond to an intermolecular process between ortho- and para-rearranged intermediate and TEA, respectively. At first, an intermolecular proton transfer occurs from the corresponding intermediate to TEA. After that, back proton transfer takes place immediately from protonated TEA to the intermediate anion to yield the final product. The enhancement of the rate for the 1,3-hydrogen shift by TEA is considerably greater than that for the 1,5-shift. This fact can be understood considering that the structure of the ortho-rearranged intermediate is more favorable

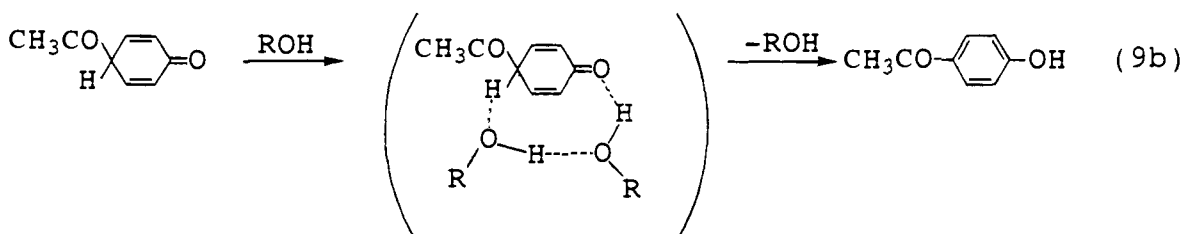
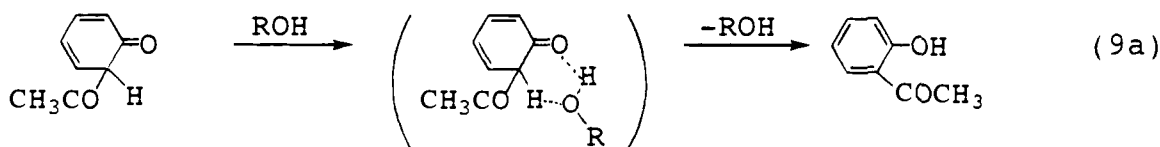
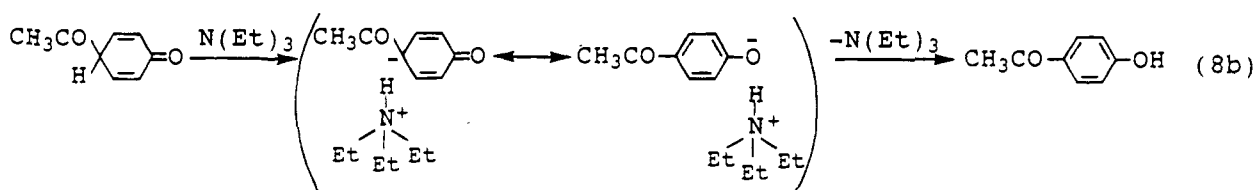
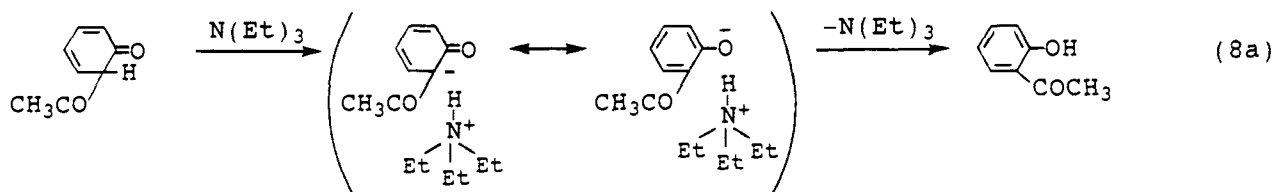
for the base-catalyzed hydrogen shift than that of the para-rearranged one as can be seen in eqs 8a and b.

In the case of alcohols, remarkable enhancement for the rates of 1,3- and 1,5-sigmatropic shifts is caused by a mutual proton exchange reaction between the rearranged intermediates and alcohol molecule(s) as shown in eqs 9a and b.

Furthermore, the results of PM3 calculations<sup>40</sup> showed that the migrating hydrogen atom in the intermediate is electronically positive for the ortho-rearranged intermediate (+0.1079) and for the para-rearranged intermediate (+0.1007). The oxygen atom of the accepting carbonyl group of the ortho or para-intermediate is electronically negative (-0.3215) or (-0.3068), respectively. As a result, the rates of the hydrogen shifts are enhanced considerably by TEA and alcohols as shown by eqs 8 and 9.

The enhancement of the rates for the 1,3- and 1,5-shifts in the relatively polar solvents, DEE and THF, is also caused similarly by a basic catalysis of the solvents. It is noteworthy that the 1,3- and 1,5-sigmatropic shifts in nonpolar MCH proceed via intramolecular processes at a low concentration of PAH or PAD.

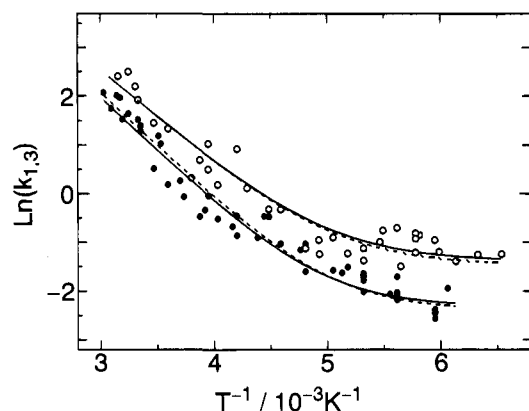
**Temperature Effects on the 1,3-Sigmatropic Hydrogen and Deuterium Shifts.** The measurements of the temperature effect on the 1,3-sigmatropic hydrogen (or deuterium) shift by 266 nm laser photolysis were carried out at a low concentration of PAH ( $2 \times 10^{-3} \text{ M}$ ) in MCH to avoid the intermolecular interactions. Figure 6 shows the plots of  $k_{1,3}^{\text{H}}$  (or  $k_{1,3}^{\text{D}}$ ) as a function of  $T^{-1}$  in MCH. The value of  $k_{1,3}^{\text{H}}$  is greater than that of  $k_{1,3}^{\text{D}}$  at each temperature, indicating that there is the isotope effect on the 1,3-sigmatropic shifts as stated above. The slopes



**Table 1.** The Rate Constants of 1,3- and 1,5-Sigmatropic Shifts of PAH and PAD<sup>a</sup>

	Solvent	$\epsilon^e$	$(k_{1,3})_{se}/M^{-1} s^{-1}$	$(k_{1,3})_{se}/M^{-1} s^{-1}$	$(k_{1,5})_0/s^{-1}$	$(k_{1,5})_{se}/M^{-1} s^{-1}$
PAH	MCH	2.0	3.6(±0.6)	$3.3(\pm 0.6) \times 10^2$	$6.5(\pm 0.6) \times 10^{-2}$	2.8(±0.7)
	ACN	37.5	$5.0(\pm 1.0) \times 10$	$5.3(\pm 1.0) \times 10^3$	$1.2(\pm 0.4) \times 10^2$	$1.1(\pm 0.2) \times 10^4$
	DEE <sup>b</sup>	4.3	$2.9(\pm 0.2) \times 10^2$		$8.8(\pm 0.6) \times 10$	
	THF <sup>b</sup>	7.6	$3.0(\pm 0.1) \times 10^2$		$1.5(\pm 0.1) \times 10$	
	MeOH	32.7	$3.0(\pm 0.4) \times 10^5$	c	$2.5(\pm 0.2) \times 10^5$	c
	EtOH	24.5	$3.3(\pm 0.5) \times 10^5$	c	$4.4(\pm 0.6) \times 10^5$	c
	1-PrOH	20.3	$2.7(\pm 0.1) \times 10^5$	c	$2.7(\pm 0.2) \times 10^5$	c
	i-PrOH	12.5	$2.8(\pm 0.2) \times 10^5$	c	$2.8(\pm 0.1) \times 10^5$	c
	TFE	26.7	$3.0(\pm 1.2) \times 10$	c	$8.2(\pm 1.1) \times 10$	c
	PAD	MCH	2.0	$9.5(\pm 0.6) \times 10^{-1}$	$8.6(\pm 1.0) \times 10$	
ACN <sup>b</sup>		37.5	$1.6(\pm 0.4) \times 10$		$4.4(\pm 0.4) \times 10$	
DEE <sup>b</sup>		4.3	$9.1(\pm 1.0) \times 10^{-1}$		1.2(±0.05)	
THF <sup>b</sup>		7.6	1.7(±0.1)		3.4(±0.05)	

<sup>a</sup> For details, see text. <sup>b</sup> In order to avoid the self-enhanced hydrogen and deuterium shifts, the rate measurements were carried out at a relatively low concentration ( $\sim 2 \times 10^{-3}$  M). <sup>c</sup> There was no self-enhancement effect on the hydrogen shift in alcohols. <sup>d</sup> The rate of 1,5-deuterium shift was too slow to measure the corresponding spectral change by laser flash photolysis in MCH. <sup>e</sup> From Isaacs N. S. *Physical Organic Chemistry* Wiley, New York, 1987, p 180.

**Figure 6.** The Arrhenius plots of the observed rates of the 1,3-hydrogen (open circle) and deuterium (closed circle) shifts of PAH and PAD in MCH. Broken lines denote the calculated rates. For details, see text.**Table 2.** Rate Parameters of 1,3-Hydrogen and Deuterium Shifts of PAH and PAD<sup>a</sup>

	$k_1/s^{-1}$	$k_2/10^3 s^{-1}$	$\Delta E^b/kcal mol^{-1}$
1,3-H Shift	$2.5 \times 10^{-1}$	4.5	3.9
1,3-D Shift	$9.9 \times 10^{-2}$	5.5	4.4

<sup>a</sup> The values were experimentally obtained. <sup>b</sup>  $\Delta E = E_v$ . For details, see text.

of the plots become small in the low temperature range  $\leq 200$  K. That is, the sigmatropic hydrogen and deuterium shifts probably proceed via quantum mechanical tunnelling in the electronically ground state.<sup>41</sup> In the high temperature range  $\geq 200$  K, the Arrhenius plots give a linear line. The observed rate of  $k_{1,3}$  ( $= k_{1,3}^H$  or  $k_{1,3}^D$ ) can be expressed by eq 10, taking into account the Boltzmann distribution between two vibrational energy levels ( $\nu = \nu_0$  and  $\nu = \nu_1$ )<sup>41</sup>

$$k_{1,3} = \frac{k_1 + k_2 \exp(-\Delta E/RT)}{1 + \exp(-\Delta E/RT)} \quad (10)$$

where  $\Delta E$  is the energy difference between the two levels, and  $k_1$  and  $k_2$  are their temperature-independent reaction rates. By the best fitting of eq 10 to the plots of  $k_{1,3}^H$  vs  $T^{-1}$  in Figure 6, the values of  $k_1^H$ ,  $k_2^H$  and  $\Delta E^H$  were determined to be  $0.25 s^{-1}$ ,  $4.5 \times 10^3 s^{-1}$  and  $3.9 kcal mol^{-1}$  for the 1,3-hydrogen shift, respectively. Similar analysis was carried out for  $k_{1,3}^D$  vs  $T^{-1}$ , and  $k_1^D$ ,  $k_2^D$  and  $\Delta E^D$  were determined as  $9.9 \times 10^{-2} s^{-1}$ ,  $5.5 \times 10^3 s^{-1}$ , and  $4.4 kcal mol^{-1}$ , respectively. These data are summarized in Table 2. The best fitted values of  $k_{1,3}$  are shown by the solid lines in Figure 6. The experimental results for both

temperature and isotope effects on  $k_{1,3}$  strongly support the tunnelling mechanism for the 1,3-sigmatropic shifts.

The temperature effects on the 1,5-sigmatropic shift in MCH were also examined. However, the rate of  $k_{1,5}^H$  in the low temperature range 270 K was too slow to measure it by laser flash photolysis.

**Theoretical Consideration for the 1,3-Sigmatropic Hydrogen and Deuterium Shifts via Tunnelling.** The theoretical treatment of the hydrogen atom transfer via tunnelling has been extensively studied by Formosinho.<sup>33-38</sup> The potential surfaces of the ortho-rearranged intermediate and ortho-final product for the 1,3-hydrogen shift were calculated by his method.<sup>33,34</sup> The force constant,  $f_r$ , of CO and CH stretching motions in the ortho intermediate was estimated by use of C=O and CH force constants ( $f_{C=O}$  and  $f_{CH}$ ) for C=O and CH stretching vibrations as follows:<sup>33-35</sup>

$$f_r^2 = f_{C=O}^2 + f_{CH}^2 + 2f_{C=O}f_{CH} \cos \theta(CO,CH) \quad (11)$$

The value of  $f_r$  for the C=O and CH system (or C=O and CD system) was obtained as  $5.48 \times 10^7 cm^{-1} nm^{-2}$  (or  $5.56 \times 10^7 cm^{-1} nm^{-2}$ ). The potential energy,  $V_r$ , for the ortho-rearranged intermediate is estimated by assuming a harmonic behavior for the two oscillators

$$V_r = \frac{1}{2} f_r x^2 \quad (12)$$

where  $x$  is the reaction coordinate, i.e., the common displacement of the CO and CH bonds. The force constant,  $f_p$ , of CO and OH stretching motions in the ortho-final product was also estimated by using the force constants,  $f_{C-O}$  and  $f_{OH}$ , of C-O and OH stretching vibrations.<sup>33-35</sup>

$$f_p^2 = f_{C-O}^2 + f_{OH}^2 - 2f_{C-O}f_{OH} \cos \theta(CO,OH) \quad (13)$$

The negative sign arises because the two oscillators vibrate out of phase, immediately after the hydrogen atom transfer. Since the motions of all the atoms are not independent, e.g.

$$x_{OH} = -(x_{CO} + x_{CH}) \quad (14)$$

all the vibrations can be considered along a common bond stretch direction. By projecting the stretching motion of the OH bond in the system of axes of the ortho-rearranged intermediate, eq 15 can be derived.<sup>33-35</sup>

$$f_p^2 = f_{C-O}^2 + f_{OH}^2 - 2f_{C-O}f_{OH} \cos \theta(CO,OH) \quad (15)$$

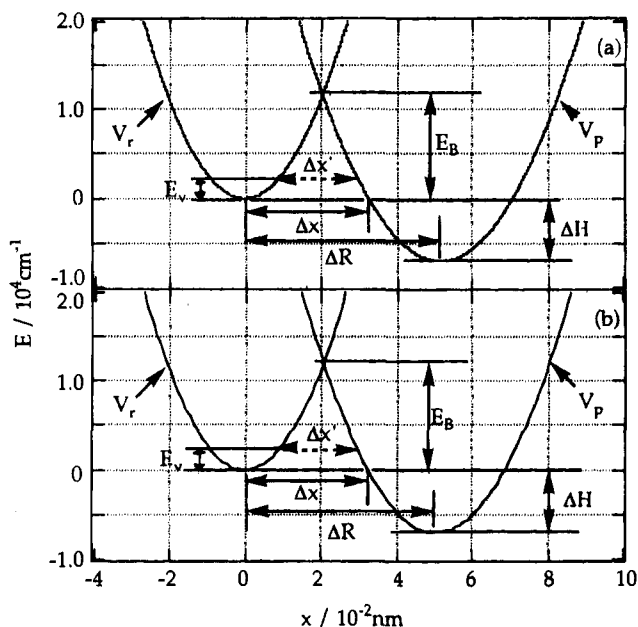


**Figure 7.** Potential energy curves of C=O and CH (or CD) oscillators in the ortho-rearranged intermediate and C-O and OH (OD) oscillators in *o*-products for the 1,3-hydrogen and deuterium shifts of PAH (a) and PAD (b). For details, see text.

where  $f_{\text{OH}} = f_{\text{OH}}[\cos \theta(\text{CO,OH}) + \cos \theta(\text{CH,OH})]$ . The values of  $f_p$  for the hydrogen and the deuterium shifted products were obtained to be  $3.81 \times 10^7$  and  $4.23 \times 10^7 \text{ cm}^{-1} \text{ nm}^{-2}$ , respectively. Here, the angle of the three displacement coordinate axes is taken as the angle,  $\theta$ , of the coordinate axes for a triatomic molecule XYZ of atomic masses  $m_1$ ,  $m_2$  and  $m_3$

$$\cos \theta = \left[ \frac{m_1 m_3}{(m_1 + m_2)(m_2 + m_3)} \right]^{1/2} \quad (16)$$

The angle between  $x_{\text{CH}}$  and  $x_{\text{CO}}$  can be estimated with  $m_1 = 1$  (for the 1,3-deuterium shift,  $m_1 = 2$ ),  $m_2 = 24$ , and  $m_3 = 16$  where  $m_2$  concentrates the mass of the two carbon atoms.

Figures 7(parts a and b) show the calculated potential energy diagrams for the 1,3-hydrogen and deuterium shifts, respectively, which are used for the theoretical consideration according to the tunnel effect theory,<sup>36</sup> where  $V_r$  and  $V_p$  denote the potential surfaces of the ortho-rearranged intermediate and ortho product, respectively,  $\Delta H$  the enthalpy change for the hydrogen shift,  $\Delta R$  the coordinate displacement,  $E_B$  the energy of crossing of the potential curves,  $E_v$  the vibrational energy for  $\nu_1$  (i.e.,  $E_v = \Delta E$ ), and  $\Delta x$  and  $\Delta x'$  the distances between the potential curves of the initial and final states at  $E = 0$  and  $E = E_v$ , respectively.

The tunnelling rate is strongly dependent on the enthalpy change,  $\Delta H$ , and on the coordinate displacement,  $\Delta R$ , between the reactant and product, because, as can be seen from Figure 7,  $\Delta x$  and to a lesser extent  $E_B$  are functions of  $\Delta H$  and  $\Delta R$ .

The energy diagram for the photo-Fries rearrangements of PAH calculated by the PM3 method<sup>40</sup> to estimate the values of  $\Delta H$  is shown in Figure 8. Here, the total heat of formation for the radical pair is calculated to be  $5.6 \text{ kcal mol}^{-1}$  from the sum of the heats of formation of acetyl ( $-5.8 \text{ kcal mol}^{-1}$ )<sup>42</sup> and phenoxyl radicals ( $11.4 \text{ kcal mol}^{-1}$ ),<sup>42</sup> and the energy level of the  $S_1$  ( $^1L_b$ ) state is known to be  $108 \text{ kcal mol}^{-1}$ .<sup>22</sup> The values of  $\Delta H$  for 1,3- and 1,5-hydrogen shifts were estimated to be

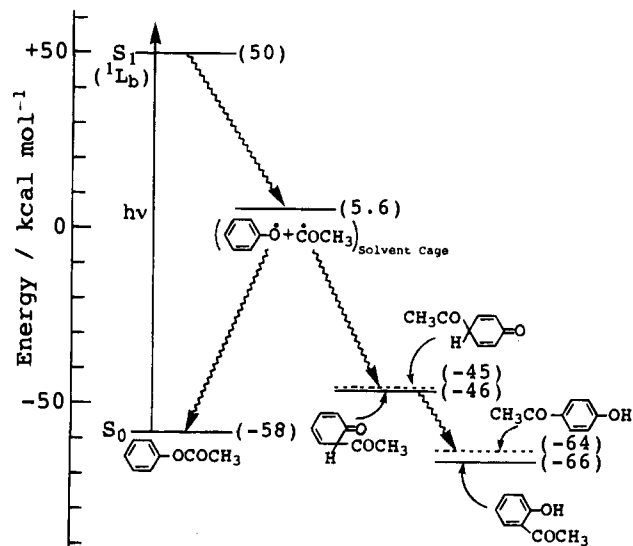


**Figure 8.** The energy diagram for the photo-Fries rearrangements of PAH calculated by the PM3 method.<sup>40</sup>

$-20$  and  $-19 \text{ kcal mol}^{-1}$ , respectively, showing that the 1,3- and 1,5-hydrogen shifts in the present system are exothermic reactions.

The potential energy of the ortho product is

$$V_p = \frac{1}{2} f_p (x - \Delta R)^2 + \Delta H \quad (17)$$

The values of  $E_B$  and  $\Delta x$  for 1,3-hydrogen shift were determined to be  $1.2 \times 10^4 \text{ cm}^{-1}$  ( $34 \text{ kcal mol}^{-1}$ ) and  $3.28 \times 10^{-2} \text{ nm}$ , respectively. The values of  $E_B$  and  $\Delta x$  for 1,3-deuterium shift were obtained as  $1.2 \times 10^4 \text{ cm}^{-1}$  and  $3.26 \times 10^{-2} \text{ nm}$ , respectively, which were very similar to those for the 1,3-hydrogen shift. According to the tunnel effect theory,<sup>36</sup> the tunnelling rate constants of  $k_{1,3}^{\text{H}}$  and  $k_{1,3}^{\text{D}}$  can be calculated by use of the values  $E_B$  and  $\Delta x$

$$k_{1,3} = \nu \exp \left\{ -\frac{2\pi}{h} [2\mu(E_B - E_v)]^{1/2} \Delta x \right\} \quad (18)$$

where  $\nu$  is the average frequency for the tunnelling (the value was assumed as  $10^{13} \text{ s}^{-1}$ ) and the value of  $E_v$  is equal to  $\Delta E$ . Here,  $\mu$  is the reduced mass estimated by eq 19<sup>33</sup>

$$\mu^{1/2} = \mu_{\text{CO}}^{1/2} + \mu_{\text{CH}}^{1/2} \quad (19)$$

where  $\mu_{\text{CO}}$  and  $\mu_{\text{CH}}$  are the reduced masses for CO and CH vibrations. At first, we tried the estimation of the  $\Delta R$  value by use of eq 20<sup>33</sup>

$$(\Delta R)^2 = r_{\text{CO}}^2 + r_{\text{XH}}^2 + 2r_{\text{CO}}r_{\text{XH}} \cos \theta(\text{CO,CH}) \quad (20)$$

The values of  $r_{\text{CO}}$ ,  $r_{\text{XH}} (= (r_{\text{CH}} + r_{\text{OH}})/2)$  and  $\cos \theta$  were  $1.33 \times 10^{-2}$ ,  $1.54 \times 10^{-1}$ , and  $1.27 \times 10^{-1} \text{ nm}$  which were determined by the PM3 method.<sup>40</sup> By use of these values, the  $\Delta R$  value was estimated as  $1.55 \times 10^{-1} \text{ nm}$ , which was very large resulting in the very slow tunnelling rate compared to the experimentally obtained one ( $k_1$ ). These parameters of  $r_{\text{CO}}$ ,  $r_{\text{XH}}$ , and  $\cos \theta$  were not appropriate for the estimation of the real value of  $\Delta R$ . The determination of the exact parameters should be made in future. Therefore, the value of  $\Delta R$  (or  $\Delta x$ ) was optimized to fit that of  $k_1^{\text{H}}$  (or  $k_1^{\text{D}}$ ) (see Table 2) for hydrogen (or deuterium) tunnelling at  $E = 0$  (i.e.,  $\nu = \nu_0$ ) by use of eq 18. The values of  $\Delta R$  (or  $\Delta x$ ) were obtained to be  $5.2 \times 10^{-2}$

(41) Bell, R. P. *The Tunnelling Effect in Chemistry*; Capman and Hall: London, 1980.

(42) *CRC Handbook of Chemistry and Physics*; CRC Press, Inc.: FL, 1981.

**Table 3.** The Rates and Parameters for 1,3-Hydrogen and Deuterium Shifts via Tunnelling<sup>a</sup>

	1,3-H Shift		1,3-D Shift	
	$\nu = 0$	$\nu = \nu_1$	$\nu = 0$	$\nu = \nu_1$
$\mu/10^{-26}$ kg	2.21 <sup>b</sup>	2.21 <sup>b</sup>	2.29 <sup>b</sup>	2.29 <sup>b</sup>
$E_v/10^4$ cm <sup>-1</sup>	1.20	1.20	1.20	1.20
$E_v/10^3$ cm <sup>-1</sup>	0	1.36	0	1.55
$\Delta R/10^{-2}$ nm	5.20	5.20	5.08	5.08
$\Delta x/10^{-2}$ nm	3.28		3.26	
$\Delta x'/10^{-2}$ nm		2.40		2.30
$k_1/s^{-1}$	$2.3 \times 10^{-1}$		$9.2 \times 10^{-2}$	
$k_2/s^{-1}$		$4.5 \times 10^3$		$6.1 \times 10^3$

<sup>a</sup> For details, see text. <sup>b</sup> Calculated by use of eq 19.

nm (or  $3.28 \times 10^{-2}$  nm) for the hydrogen tunnelling and  $5.08 \times 10^{-2}$  nm (or  $3.26 \times 10^{-2}$  nm) for the deuterium tunnelling.

The value of  $\Delta R$  for the hydrogen tunnelling was also evaluated by use of intersecting-state model (ISM) proposed by Formosinho.<sup>34</sup> The ISM expression required to estimate the sum of the bond extensions to the transition state is

$$d = \frac{a' \ln 2}{n^\ddagger} (r_p + r_r) \quad (21)$$

where  $a'$  is a constant ( $= 0.156$ ),  $r_p$  and  $r_r$  are the equilibrium bond lengths of product and reactant, and  $n^\ddagger$  is the transition-state bond order. In the present system, there are two kinds of bond rearrangements: for H (CH to OH) and O (C=O to C-O). So the sum of bond extensions ( $d = \Delta R$ ) is taken as the average of the two bond extensions  $d_{XH}$  and  $d_{CO}$ . There is the bond rearrangement for H-migration, involving a CH and a OH bond through a bond-breaking-bond-forming process. The transition-state bond order is  $n^\ddagger = 0.5$ , and

$$d_{XH} = \frac{a' \ln 2}{0.5} (r_{CH} + r_{OH}) \quad (22)$$

There is also the CO rearrangement that involves a breaking process C=O to C-O. The transition-state bond order is  $n^\ddagger = 0.5$ , and

$$d_{CO} = \frac{a' \ln 2}{0.5} (r_{C=O} + r_{C-O}) \quad (23)$$

The values of the bond length are  $r_{CH} = 1.09 \times 10^{-1}$ ,  $r_{OH} = 9.7 \times 10^{-2}$ ,  $r_{C=O} = 1.215 \times 10^{-1}$ , and  $r_{C-O} = 1.43 \times 10^{-1}$  nm. These values are substituted into eqs 22 and 23, and then  $d_{XH} = 4.45 \times 10^{-2}$ ,  $d_{CO} = 5.71 \times 10^{-2}$  nm, and  $\Delta R = (d_{XH} + d_{CO})/2 = 5.08 \times 10^{-2}$  nm. This value of  $\Delta R$  is close to the adjusted one ( $5.20 \times 10^{-2}$  nm) as described above. This fact shows that the present estimation of  $\Delta R$  is useful for the construction of the potential energy curves of the tunnelling process.

The values of  $\Delta x'$  at  $E = E_v (= \Delta E)$  were obtained to be  $2.40 \times 10^{-2}$  nm for the hydrogen shift and  $2.30 \times 10^{-2}$  nm for the deuterium shift. These parameters are listed in Table 3. By use of eq 18, the tunnelling rate constants,  $k_1$ , for 1,3-hydrogen and deuterium shifts at  $E = 0$  (i.e.,  $\nu = \nu_0$ ) were calculated to be  $2.3 \times 10^{-1}$  and  $9.2 \times 10^{-2}$  s<sup>-1</sup>, respectively. For the 1,3-hydrogen and deuterium shifts at  $E = E_v$  (i.e.,  $\nu = \nu_1$ ), the values of  $k_2$  were obtained as  $4.5 \times 10^3$  and  $6.1 \times 10^3$

s<sup>-1</sup>, respectively, by use of eq 18 with the above values of  $\Delta x$ . These data are also summarized in Table 3. By use of these parameters the values of  $k_{1,3}$  for the 1,3-sigmatropic hydrogen and deuterium shifts at various temperatures were calculated by eqs 10 and 18, which were plotted by broken lines in Figure 6. The calculated values of  $k_{1,3}$  agree with the experimental ones. It is concluded that the intramolecular 1,3-sigmatropic hydrogen (or deuterium) shift proceeds via tunnelling processes at both  $E = 0$  ( $\nu = \nu_0$ ) and  $E = E_v (= 3.9$  kcal mol<sup>-1</sup> for the hydrogen shift and  $4.4$  kcal mol<sup>-1</sup> for the deuterium shift) ( $\nu = \nu_1$ ) under the experimental condition.

### Concluding Remarks

(1) The rate constants for the 1,3- and 1,5-sigmatropic hydrogen (or deuterium) shifts of the photo-Fries rearranged intermediates of phenyl acetate produced by laser flash photolysis at 266 nm are directly measured in several solvents. The rate constant for the intramolecular 1,3-hydrogen shift ( $3.6$  s<sup>-1</sup>) is greater than that for the 1,5-hydrogen shift ( $6.5 \times 10^{-2}$  s<sup>-1</sup>) in the ground state in MCH at 293 K. The Woodward-Hoffmann rule cannot be applied to 1,3- and 1,5-sigmatropic hydrogen shifts in the ground state of the photo-Fries rearranged intermediates. The Woodward-Hoffmann rule is usually applicable to sigmatropic shifts in pure  $\pi$ -electron systems. However, in the present system, the intermediates have a heteroatom (carbonyl-oxygen atom) as the reactive position, so that the nonbonding electrons on the corresponding carbonyl-oxygen atom may play an important role for the sigmatropic hydrogen shifts.

(2) By use of the tunnel effect theory proposed by Formosinho,<sup>33-38</sup> potential surfaces are estimated assuming a harmonic behavior for the two oscillators. The tunnelling rate constants,  $k_{1,3}^H$  and  $k_{1,3}^D$ , can be calculated by use of the values  $E_B$  (the energy of crossing of the reactant and product potential curves) and  $\Delta x$  (the distance between the potential curves of the initial and final states). The experimental values of  $k_{1,3}$  agree with the calculated ones for the intramolecular 1,3-sigmatropic hydrogen (or deuterium) shift via tunnelling.

(3) On the basis of the experimental and theoretical results of temperature and isotope effects, it is shown that the intramolecular 1,3-hydrogen (or deuterium) shift in MCH proceeds via tunnelling processes at two vibrational energy levels:  $E = 0$  ( $\nu = \nu_0$ ) and  $E = E_v (= 3.9$  kcal mol<sup>-1</sup> for the hydrogen shift or  $4.4$  kcal mol<sup>-1</sup> for the deuterium shift) ( $\nu = \nu_1$ ) under the experimental condition.

(4) The rate constants of the sigmatropic shifts are enhanced by polar solvents, especially, by alcohols. It is shown that the enhancement of the rates for the 1,3- and 1,5-sigmatropic hydrogen (or deuterium) shifts in the polar solvents is caused by a basic catalysis of the solvents. It is noteworthy that the 1,3- and 1,5-sigmatropic hydrogen shifts in nonpolar MCH proceed via the intramolecular process at a low concentration of PAH ( $\sim 2 \times 10^{-3}$  M).

**Acknowledgment.** This work was supported by a Grant-in-Aid on Priority-Area-Research: Photoreaction Dynamics (06239101) from the Ministry of Education, Science and Culture of Japan.

JA943692Y